Direct Measurement of Electron Intervalley Relaxation in a Si/Si-Ge Quantum Dot

Nicholas E. Penthorn,[1] Joshua S. Schoenfield,[1] Lisa F. Edge,[2] and HongWen Jiang[1,*]

[1] *Department of Physics & Astronomy, University of California, Los Angeles, Los Angeles, California 90095, USA*
[2] *HRL Laboratories, LLC, Malibu, California 90265, USA*

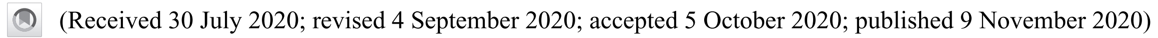

(Received 30 July 2020; revised 4 September 2020; accepted 5 October 2020; published 9 November 2020)

The presence of nondegenerate valley states in silicon can drastically affect electron dynamics in silicon-based heterostructures, leading to electron spin relaxation and spin-valley coupling. In the context of solid-state spin qubits, it is important to understand the interplay between spin and valley degrees of freedom to avoid or alleviate these decoherence mechanisms. Here we report the observation of relaxation from the excited valley state to the ground state in a Si/Si-Ge quantum dot at zero magnetic field. Valley-state readout is aided by a valley-dependent tunneling effect, which we attribute to valley-orbit coupling. We find a long intervalley relaxation time of 12.0 ± 0.3 ms, a value that is unmodified when a magnetic field is applied. Furthermore, we compare our findings with the spin relaxation time and find that the spin-valley "hot spot" relaxation is roughly 4 times slower than intervalley relaxation, consistent with established theoretical predictions. The precision of this technique, adapted from electron spin readout via energy-dependent tunneling, is an improvement over indirect valley relaxation measurements and could be a useful probe of valley physics in spin-qubit and valley-qubit implementations.

DOI: 10.1103/PhysRevApplied.14.054015

I. INTRODUCTION

Valley physics has been the subject of many theoretical and experimental studies in silicon-based quantum-dot devices, largely in association with semiconductor quantum computing [1–4]. Although the six valleys in the silicon conduction band are degenerate in the bulk crystal [5], electron confinement in quantum-dot heterostructures lifts the degeneracy and leads to two low-lying valley states, one of which is the ground state for electrons confined within the quantum-dot potential [6–9]. Out-of-plane confinement created by gate-generated electric fields and the quantum-well interface, in addition to interface disorder, determines the magnitude of the energy splitting between the two valleys [10–12]. The presence of these states is generally considered to be a hinderance to the performance of electron spin qubits in silicon, in part because noise sources can couple to spin states via the valley degree of freedom to give rise to spin relaxation [13–15]. Moreover, the spin-qubit operation point must be carefully chosen to avoid the fast-relaxation "hot spot" where the spin and valley states mix [13–16].

Several studies have found theoretically that spin relaxation in silicon is dominated by spin-valley hybridization effects at external fields used for spin quantum computing, $B_{\mathrm{ext}} \approx 0.2 - 2$ T. In this regime, the (intravalley) spin relaxation rate depends on the intervalley relaxation rate Γ_v as well as the proximity of the Zeeman-level splitting to the valley splitting E_{VS} [13]:

$$\Gamma_{\mathrm{spin}} = \frac{\sqrt{\delta^2 + \Delta_a^2} + |\delta|}{2\sqrt{\delta^2 + \Delta_a^2}} \Gamma_v. \quad (1)$$

In (1), $\delta = E_Z - E_{\mathrm{VS}}$ is the difference between the Zeeman and valley-splitting energies and Δ_a is the spin-valley coupling strength. Importantly, the intervalley relaxation rate Γ_v has polynomial growth with the magnitude of the valley splitting, with Johnson noise contributing a linear dependence and the valley-phonon interaction adding a E_{VS}^5 dependence [14–17]. In Si/SiO_2 quantum dots, E_{VS} can range from 0.1 to 1 meV [18,19] and Γ_v is expected to be as great as 100 MHz [13,17]. Consequently, a direct measurement of intervalley relaxation in quantum dots has never been achieved, as the relaxation rate is just outside the bandwidth of state-of-the-art charge detection with rf reflectometry [20–22] and far outside the bandwidth of standard capacitive charge-sensing measurements. However, the valley splitting in Si/Si-Ge-based quantum dots is almost universally smaller than that in their Si/SiO_2 counterparts [23–27] and could result in a relaxation rate slow enough to be captured in real time. This work uses a small valley $E_{\mathrm{VS}} \approx 40$ μeV found in a Si/Si-Ge quantum-dot device to directly observe intervalley relaxation with no applied magnetic fields and show that the measured

*jiangh@physics.ucla.edu

 © 2020 American Physical Society

relaxation time $T_1 = 1/\Gamma_v$ is consistent with indirect measurements extracted from spin relaxation in the vicinity of the spin-valley "hot spot." Robust readout of the valley occupation despite the small energy splitting is aided by valley-dependent tunneling, possibly originating from valley-orbit coupling. We then show that intervalley relaxation and spin relaxation can be seen at the same magnetic field value when the quantum-dot energy is modified slightly. Valley T_1 is found to be independent of the magnetic field, implying a similarly field-independent valley splitting and negligible contributions from second-order relaxation processes.

II. DEVICE CHARACTERIZATION

The device under study is a gate-defined double quantum dot fabricated on a Si/Si-Ge wafer known from earlier work to have small valley splitting [28] [Fig. 1(a)]. Positive voltage on a global accumulation gate creates a two-dimensional electron gas and voltages on local depletion gates define potential wells in the plane of the wafer. A single-electron transistor (SET) formed in the upper channel is used to detect changes in electron occupation of the two quantum dots, defined in the lower channel. For this work, interdot tunneling is suppressed by our setting an appropriately negative voltage on barrier gate M, effectively creating two noninteracting charge boxes that are each coupled to separate electron reservoirs. The dots' energy can be controlled with voltages on plunger gates L and R, and the rates of electron tunneling into and out of each reservoir are controlled with barrier gate voltages on BL and BR. Both quantum-dot energies are tuned to the single-electron limit, so that at any point during experiments there is either one electron or zero electrons in each dot [Fig. 1(b)]. Dot occupation is confirmed by magnetospectroscopy [29]. We focus on the right dot since the valley splitting in the left dot was found previously to be around 20 μeV [28], which is too small to perform valley readout with our system.

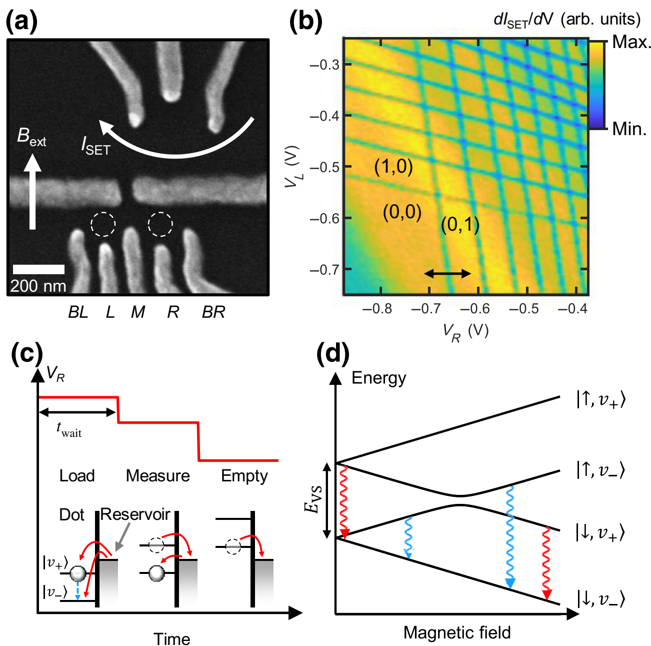

FIG. 1. Device characterization and measurement details. (a) Scanning electron micrograph of the double-dot device. Arrows represent the direction of current through the single-electron transistor I_{SET} and the applied magnetic field B_{ext}, where applicable. (b) Charge-stability diagram of the double quantum dot with interdot tunneling suppressed. Indices (i, j) indicate the occupation of the (right, left) dot. The black arrow shows the location of voltage pulses on gate R. (c) The three-stage pulse used to convert spin-valley-state occupation to a SET current signal. During the "load" stage, an electron in the excited valley can relax to the ground state. (d) Spin-valley levels as a function of in-plane magnetic field, including the relaxation mechanisms probed in this study: intervalley (red arrows) and spin (blue arrows).

III. MEASURING VALLEY-STATE OCCUPATION

Conversion of single-electron valley-state occupation to charge for SET readout is accomplished in real time by use of energy-dependent tunneling [30–32]. A three-stage voltage pulse modifies the dot energy as shown in Fig. 1(c). First an electron is loaded into the dot from the reservoir and held there for time t_{wait}. Assuming reservoir electrons occupy both valley states evenly, the loaded electron will occupy the excited valley or the ground valley with probabilities determined by the tunnel-in rates associated with both states. In the measurement phase of the pulse, the dot energy is raised so that the valley states straddle the reservoir Fermi level. If the loaded electron is in the excited valley at the beginning of this phase, it can tunnel into the reservoir and tunnel back into the dot's ground state, registering as an abrupt and transient increase in SET current. The principle of this operation is the same as the technique commonly used for measuring single spin relaxation, except here the measurement occurs at zero applied magnetic field so that the Zeeman splitting is much smaller than the valley splitting and the readout level lies between valley states, not spin states [see Fig. 1(d) for relaxation processes that can be observed with this technique]. In our device the valley splitting seen in both dots is comparable to thermal broadening, so we analyze valley occupation with 2000 averages of the pulse sequence. When averaged, the random transient signal generated by an excited state electron becomes a "tunneling peak" that can be easily discriminated from thermally driven random telegraph signal [33]. The SET current, which contains the electron response to the pulse and a comparable component that arises from the capacitive coupling of the pulsed gate to the SET, can be converted to a probability of the dot being unoccupied. This is accomplished by our performing an identical three-stage pulse far enough away from the

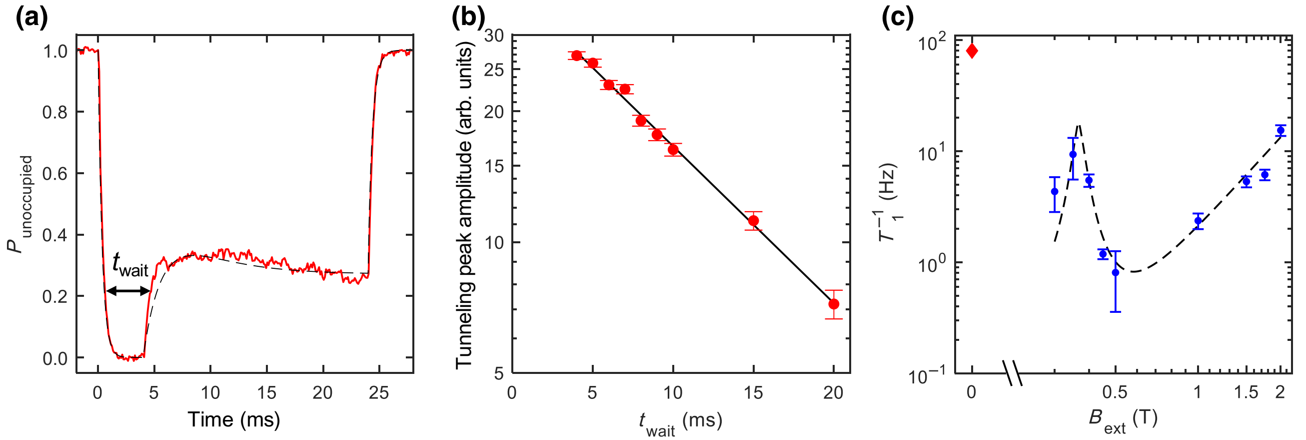

FIG. 2. Valley and spin relaxation. (a) Probability of the right dot being unoccupied during the pulse sequence with $t_{\mathrm{wait}} = 4\,\mathrm{ms}$. The tunneling peak is visible during the readout pulse stage, indicating upper-valley-state occupation. The dotted black line is the fit to rate-equation model. (b) Tunneling peak amplitude as a function of time spent in the load stage t_{wait}. The trend follows an exponential decay with valley $T_1 = 12.0 \pm 0.3\,\mathrm{ms}$. (c) Blue circles indicate the spin relaxation rate at nonzero fields shows a hot spot at $B_{\mathrm{ext}} = 0.37 \pm 0.03\,\mathrm{T}$, where spin and valley states mix. The red diamond represents the intervalley relaxation rate $\Gamma_v = 1/T_1 = 83 \pm 2\,\mathrm{Hz}$ at zero field. The error bar is smaller than the diamond and is not shown.

charge transition such that no electron tunneling occurs. The resulting SET current contains only the capacitive coupling to the pulsed gate and can be subtracted from the original data to reveal the pure electron response to the pulse. Then, provided the "load" and "empty" stages of the pulse are long enough compared with the electron tunneling rates, the electron response can be scaled so that the unoccupied probability is 0 at the end of the "load" stage and 1 at the end of the "empty" stage. Figure 2(a) shows the probability of the right dot to be empty over the three-step pulse, with a tunneling peak appearing in the measurement phase. Remarkably, the tunnel-in and tunnel-out rates contributing to the valley tunneling peak are much lower than the rates associated with the electron loading and unloading pulse stages. Modelling the probability of dot occupation with coupled classical rate equations and taking thermal effects into account [34,35], we find the slow electron hopping that constitues the tunneling peak can be fully explained by a dependence of the tunneling rate on the occupied state, temperature and the direction of tunneling.

IV. INTERVALLEY RELAXATION

Because any electron loaded into the dot's excited valley can decay to the ground state in the presence of intervalley relaxation, the amplitude of the tunneling peak will decrease exponentially as a function of t_{wait} with a characteristic relaxation time T_1 as $e^{-t_{\mathrm{wait}}/T_1}$. Figure 2(b), which is the main result of this paper, shows the direct observation of intervalley relaxation with a valley T_1 of 12.0 ± 0.3 ms. As expected from the small valley splitting, this value is long when compared with previous estimates in $\mathrm{Si/SiO_2}$ and Si/Si-Ge [13,24].

A direct comparison between spin and valley relaxation is made by our repeating the T_1 measurement at nonzero applied magnetic field, in the limit where the Zeeman splitting is comparable to or larger than the valley splitting. Plotting the spin relaxation rate as a function of the field reveals the well-studied hot spot where the Zeeman and valley levels mix [Fig. 2(c)]. Relaxation at the spin-valley anticrossing increases sharply and is expected to be on the order of the bare-valley relaxation, shown by our setting $\delta = 0$ in Eq. (1). We find a hot spot at 0.37 ± 0.03 T in the right dot, corresponding to $E_{\mathrm{VS}} = 43 \pm 4\,\mu\mathrm{eV}$, consistent with previous measurements obtained from Ramsey-fringe experiments on the same device [28]. From a fitting of the relaxation curve, including phonon-noise and Johnson-noise contributions [14–16,36], we find that the relaxation rate at the anticrossing is approximately 20 Hz, which is roughly a quarter of the intervalley rate measured at zero field. Taking into consideration the imprecision of the hot-spot location from the fit, the hot-spot relaxation rate is fairly close to the expected value of $2/T_1 \approx 40\,\mathrm{Hz}$. Thus, the spin relaxation time at the hot spot can be used as an indirect, albeit imprecise, measurement to confirm the intervalley relaxation time.

V. VALLEY-DEPENDENT TUNNELING

Fitting the valley tunneling peaks to the rate-equation model reveals that the tunneling rate out of the excited valley state differs from the rate out of the ground state by a factor of 4 (i.e., $\Gamma_{v+}^{\mathrm{out}}/\Gamma_{v-}^{\mathrm{out}} \approx 4$). To support this discovery, we find that the readout window for measuring valley occupation is twice the valley splitting. In the case where all tunneling rates are equal in the measurement stage, we would expect valley readout only when

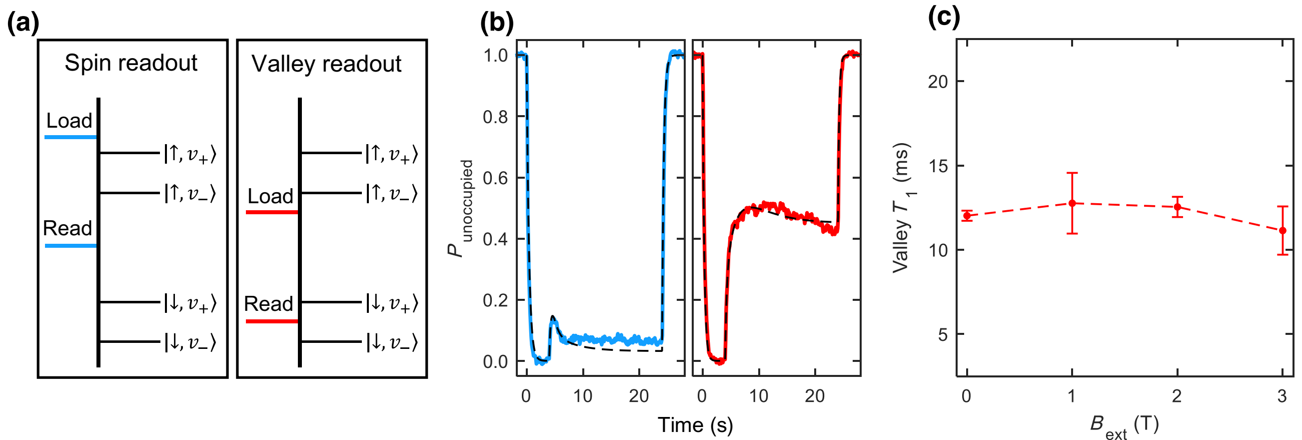

FIG. 3. Reading out spin and valley states together at nonzero magnetic field. (a) The possible modes of state readout when the Zeeman energy is greater than the valley splitting. In the left panel the "load" pulse level is above all relevant dot states and the "read" level is between spin states. In the right panel the "load" level is below the excited spin state and the "read" level is between valley states. (b) Example of spin-discriminating tunneling peak (left) and valley-discriminating tunneling peak (right) at $B_{\text{ext}} = 2\,\text{T}$, accomplished by our uniformly moving all pulse stage energies. Dotted lines represent an approximate fit to a four-state rate-equation model. (c) The intervalley relaxation time is shown to be independent of the magnetic field to within the error bars.

the reservoir Fermi level is between valley states, and an extended readout window is possible only when the tunneling rates associated with the two dot states are different. A likely explanation for valley-dependent tunneling is valley-orbit coupling, which under certain conditions leads to shifts in the orbital envelope functions of the two valleys [37]. This explanation is conceivable given the small valley splitting observed and the interdot valley coupling seen in this device [28]. To obtain a qualitative estimate of valley-dependent tunneling from valley-orbit coupling, we calculate the wave functions of the lowest two dot states in the presence of interface disorder using a disorder-expansion effective-mass approach developed in Ref. [38]. In the presence of a single step at the Si/Si-Ge interface to introduce valley-orbit coupling, the excited valley wave function is laterally shifted with respect to the ground state and valley-dependent tunneling is expected with $\Gamma^{\text{out}}_{v_+}/\Gamma^{\text{out}}_{v_-} = 6.4$ [34]. Of course, since we cannot know the atomic scale details of the device heterostructure, the true origin of valley-orbit coupling may not be a single interface step; however, the step model allows comparison with other theoretical studies that investigate valley-orbit coupling in quantum dots and provides a qualitative explanation for the observed effect.

VI. SPIN AND VALLEY READOUT AT NONZERO FIELD

Lastly, the effects of a magnetic field on intervalley relaxation are investigated. This is achieved by our fixing the relative energies of the load, read and empty pulse stages and shifting them all uniformly with plunger gate voltage V_R. In the region above the spin-valley anticrossing where $E_z > E_{\text{VS}}$, both spin and valley tunneling peaks are observable. They can be addressed separately by setting the load level to be sufficiently small and varying V_R through the charge transition. At lower dot energies where the read level straddles spin states, the spin occupation is read out. When the dot energy is increased to the point where the read level straddles valley states and the load level is below the excited spin state, valley occupation can be measured [Fig. 3(a)]. Consistent with the zero-field results, the valley tunneling peak is on a longer timescale than the spin tunneling peak [Fig. 3(b)]. This discrepancy can again be explained by considering the exponential dependence of dot-reservoir tunneling rates on the dot energy [15,39]. Generally, as the levels involved in the tunneling peak become further apart, the associated tunneling rates diverge. Comparison of the two tunneling peaks with the rate-equation model, now including all four spin-valley states, shows good qualitative agreement [34]. Intervalley relaxation is found to be independent of field to within the error bars, confirming that single-phonon processes are the dominant relaxation mechanism despite the electron temperature being comparable to the valley splitting [Fig. 3(c)]. This measurement also verifies that the states involved in the relaxation process are field independent, as the valley states should be.

VII. DISCUSSION

The valley T_1 in our device is 12 ms, which is long enough to have consequences for qubit operation. As we have shown, the long intervalley relaxation is constant through the magnetic field range used for a typical spin

qubit. In this context, a valley relaxation time that is longer than the spin operation time (typically a few microseconds) could be detrimental, as quantum information will leak into the excited valley state and remain there during operations. On the other hand, the slow intervalley relaxation times seen here are a reflection of weak coupling to noise sources, meaning that a system with long valley T_1 also has long spin relaxation times. A direct measurement of real-time valley dynamics could therefore be of use for spin-qubit characterization. For valley-qubit implementations [28,40,41], small valley splittings that can be easily addressed with microwave excitations together with a long valley T_1 are highly desirable. The presence of valley-dependent tunneling that allows an extended readout window beyond $E_{\mathrm{VS}} \approx 43\,\mu\mathrm{eV}$ could also be a beneficial enhancement of valley-qubit measurement fidelity.

Considering the expected strong dependence of valley T_1 on the magnitude of the valley splitting, it would be beneficial to repeat the measurements here while modifying the quantum-dot position within the interface disorder-potential landscape to change E_{VS}. In principle this could be achieved by biasing gate M to be more positive and biasing gate BR to be more negative, for example. In practice, we can resolve the valley tunneling peak only for a small range of side-gate voltages, corresponding to negligible changes to the valley splitting. This is because the dot-reservoir tunneling rates, and therefore the tunneling peak, are highly sensitive to V_{BR}.

VIII. CONCLUSION

We directly observe relaxation from the excited valley state to the ground state at zero magnetic field in real time, made possible by the small valley splitting—and therefore a slow relaxation rate—in a Si/Si-Ge quantum dot. Because of valley-dependent tunneling, possibly arising from valley-orbit coupling, there is an extended window for reading out valley states that allows reliable measurements even when the thermal energy and valley splitting are comparable. From the field independence of the relaxation, we can conclude that the valley splitting is unchanged by in-plane magnetic fields and higher-order relaxation processes are negligible up to $B_{\mathrm{ext}} = 3\,\mathrm{T}$. The demonstrated method of intervalley relaxation measurement is as precise as single-spin T_1 measurements by nature, and could prove useful as a characterization tool for spin and valley qubits in silicon.

ACKNOWLEDGMENTS

This work was supported by the U.S. Army Research Office through Grant No. W911NF1410346. N.E.P acknowledges support from the Julian Schwinger Graduate Fellowship at the University of California, Los Angeles.

[1] D. Loss and D. P. DiVincenzo, Quantum computation with quantum dots, Phys. Rev. A **57**, 120 (1998).

[2] J. J. Pla, K. Y. Tan, J. P. Dehollain, W. H. Lim, J. J. L. Morton, D. N. Jamieson, A. S. Dzurak, and A. Morello, A single-atom electron spin qubit in silicon, Nature **489**, 541 (2012).

[3] M. Veldhorst, C. H. Yang, J. C. C. Hwang, W. Huang, J. P. Dehollain, J. T. Muhonen, S. Simmons, A. Laucht, F. E. Hudson, K. M. Itoh, A. Morello, and A. S. Dzurak, A two-qubit logic gate in silicon, Nature **526**, 410 (2015).

[4] J. Yoneda, K. Takeda, T. Otsuka, T. Nakajima, M. R. Delbecq, G. Allison, T. Honda, T. Kodera, S. Oda, Y. Hoshi, N. Usami, K. M. Itoh, and S. Tarucha, A quantum-dot spin qubit with coherence limited by charge noise and fidelity higher than 99.9%, Nat. Nanotechnol. **13**, 102 (2018).

[5] T. Ando, A. B. Fowler, and F. Stern, Electronic properties of two-dimensional systems, Rev. Mod. Phys. **54**, 437 (1982).

[6] F. Schaffler, High-mobility Si and Ge structures, Semicond. Sci. Technol. **12**, 1515 (1997).

[7] D. Culcer, L. Cywinski, Q. Li, X. Hu, and S. D. Sarma, Quantum dot spin qubits in silicon: Multivalley physics, Phys. Rev. B **82**, 155312 (2010).

[8] A. L. Saraiva, M. J. Calderon, R. B. Capaz, X. Hu, S. D. Sarma, and B. Koiller, Intervalley coupling for interface-bound electrons in silicon: An effective mass study, Phys. Rev. B **84**, 155320 (2011).

[9] F. A. Zwanenburg, A. S. Dzurak, A. Morello, M. Y. Simmons, L. C. L. Hollenberg, G. Klimeck, S. Rogge, S. N. Coppersmith, and M. A. Eriksson, Silicon quantum electronics, Rev. Mod. Phys. **85**, 961 (2013).

[10] S. Goswami, K. A. Slinker, M. Friesen, L. M. McGuire, J. L. Truitt, C. Tahan, L. J. Klein, J. O. Chu, P. M. Mooney, D. W. V. D. Weide, R. Joynt, S. N. Coppersmith, and M. A. Eriksson, Controllable valley splitting in silicon quantum devices, Nat. Phys. **3**, 41 (2007).

[11] M. O. Nestoklon, L. E. Golub, and E. L. Ivchenko, Spin and valley-orbit splittings in SiGe/Si heterostructures, Phys. Rev. B **73**, 235334 (2006).

[12] M. Friesen, S. Chutia, C. Tahan, and S. N. Coppersmith, Valley splitting theory of SiGe/Si/SiGe quantum wells, Phys. Rev. B **75**, 115318 (2007).

[13] C. H. Yang, A. Rossi, R. Ruskov, N. S. Lai, F. A. Mohiyaddin, S. Lee, C. Tahan, G. Klimeck, A. Morello, and A. S. Dzurak, Spin-valley lifetimes in a silicon quantum dot with tunable valley splitting, Nat. Commun. **4**, 2069 (2013).

[14] P. Huang and X. Hu, Spin relaxation in a Si quantum dot due to spin-valley mixing, Phys. Rev. B **90**, 235315 (2014).

[15] L. Petit, J. M. Boter, H. G. J. Eenink, G. Droulers, M. L. V. Tagliaferri, R. Li, D. P. Franke, K. J. Singh, J. S. Clarke, R. N. Schouten, V. V. Dobrovitski, L. M. K. Vandersypen, and M. Veldhorst, Spin Lifetime and Charge Noise in hot Silicon Quantum dot Qubits, Phys. Rev. Lett. **121**, 076801 (2018).

[16] F. Borjans, D. M. Zajac, T. M. Hazard, and J. R. Petta, Single-Spin Relaxation in a Synthetic Spin-Orbit Field, Phys. Rev. Appl. **11**, 044063 (2019).

[17] C. Tahan and R. Joynt, Relaxation of excited spin, orbital, and valley qubit states in ideal silicon quantum dots, Phys. Rev. B **89**, 075302 (2014).
[18] M. Veldhorst, J. C. C. Hwang, C. H. Yang, A. W. Leenstra, B. D. Ronde, J. P. Dehollain, J. T. Muhonnen, F. E. Hudson, K. M. Itoh, A. Morello, and A. S. Dzurak, An addressable quantum dot qubit with fault-tolerant control fidelity, Nat. Nanotechnol. **9**, 981 (2014).
[19] J. K. Gamble, P. Harvey-Collard, N. T. Jacobson, A. D. Baczewski, E. Nielsen, L. Maurer, I. Montano, M. Rudolph, M. S. Carroll, C. H. Yang, A. Rossi, A. S. Dzurak, and R. P. Muller, Valley splitting of single-electron Si MOS quantum dots, Appl. Phys. Lett. **109**, 253101 (2016).
[20] C. Barthel, M. Kjaergaard, J. Medford, M. Stopa, C. M. Marcus, M. P. Hanson, and A. C. Gossard, Fast sensing of double-dot charge arrangement and spin state with a radio-frequency sensor quantum dot, Phys. Rev. B **81**, 161308(R) (2010).
[21] J. I. Colless, A. C. Mahoney, J. M. Hornibrook, A. C. Doherty, H. Lu, A. C. Gossard, and D. J. Reilly, Dispersive Readout of a few-Electron Double Quantum dot with Fast rf Gate Sensors, Phys. Rev. Lett. **110**, 046805 (2013).
[22] T. Y. Han, M. B. Chen, G. Cao, H. O. Li, M. Xiao, and G. P. Guo, Radio-frequency measurement in semiconductor quantum computation, Sci. China - Phys. Mech. Astron. **60**, 057301 (2017).
[23] M. G. Borselli, R. S. Ross, A. A. Kiselev, E. T. Croke, K. S. Holabird, P. W. Deelman, L. D. Warren, I. Alvarado-Rodriquez, I. Milosavljevic, F. C. Ku, W. S. Wong, A. E. Schmitz, M. Sokolich, M. F. Gyure, and A. T. Hunter, Measurement of valley splitting in high-symmetry Si/SiGe quantum dots, Appl. Phys. Lett. **98**, 123118 (2011).
[24] E. Kawakami, P. Scarlino, D. R. Ward, F. R. Braakman, D. E. Savage, M. G. Lagally, M. Friesen, S. N. Coppersmith, M. A. Eriksson, and L. M. K. Vandersypen, Electrical control of a long-lived spin qubit in a Si/SiGe quantum dot, Nat. Nanotechnol. **9**, 666 (2014).
[25] D. M. Zajac, T. M. Hazard, X. Mi, K. Wang, and J. R. Petta, A reconfigurable gate architecture for Si/SiGe quantum dots, Appl. Phys. Lett. **106**, 223507 (2015).
[26] X. Mi, C. G. Peterfalvi, G. Burkard, and J. R. Petta, High-resolution Valley Spectroscopy of Si Quantum Dots, Phys. Rev. Lett. **119**, 176803 (2017).
[27] J. S. Schoenfield, B. M. Freeman, and H. Jiang, Coherent manipulation of valley states at multiple charge configurations of a silicon quantum dot device, Nat. Commun. **8**, 64 (2017).
[28] N. E. Penthorn, J. S. Schoenfield, J. D. Rooney, L. F. Edge, and H. Jiang, Two-axis quantum control of a fast valley qubit in silicon, Npj Quantum Inf. **5**, 94 (2019).
[29] W. H. Lim, C. H. Yang, F. A. Zwanenburg, and A. S. Dzurak, Spin filling of valley-orbit states in a silicon quantum dot, Nanotechnology **22**, 335704 (2011).
[30] J. M. Elzerman, R. Hanson, L. H. W. V. Beveren, B. Witkamp, L. M. K. Vandersypen, and L. P. Kouwenhoven, Single-shot read-out of an individual electron spin in a quantum dot, Nature **430**, 431 (2004).
[31] A. Morello, J. J. Pla, F. A. Zwanenburg, K. W. Chan, K. Y. Tan, H. Huebl, M. Mottonen, C. D. Nugroho, C. Yang, J. A. V. Donkelaar, A. D. C. Alves, D. N. Jamieson, C. C. Escott, L. C. L. Hollenberg, R. G. Clark, and A. S. Dzurak, Single-shot readout of an electron spin in silicon, Nature **467**, 687 (2010).
[32] C. B. Simmons, J. R. Prance, B. J. V. Bael, T. S. Koh, Z. Shi, D. E. Savage, M. G. Lagally, R. Joynt, M. Friesen, S. N. Coppersmith, and M. A. Eriksson, Tunable Spin Loading and T1 of a Silicon Spin Qubit Measured by Single-Shot Readout, Phys. Rev. Lett. **106**, 156804 (2011).
[33] M. Xiao, M. G. House, and H. W. Jiang, Measurement of the Spin Relaxation Time of Single Electrons in a Silicon Metal-Oxide-Semiconductor-Based Quantum dot, Phys. Rev. Lett. **104**, 096801 (2010).
[34] See Supplemental Material at http://link.aps.org/supplemental/10.1103/PhysRevApplied.14.054015 for tunneling peak modeling and valley wave-function calculations.
[35] E. Bonet, M. M. Deshmukh, and D. C. Ralph, Solving rate equations for electron tunneling via discrete quantum states, Phys. Rev. B **65**, 045317 (2002).
[36] A. Hollman, T. Struck, V. Langrock, A. Schmidbauer, F. Schauer, T. Leonhardt, K. Sawano, H. Riemann, N. V. Abrosimov, D. Bougeard, and L. R. Schreiber, Large, Tunable Valley Splitting and Single-Spin Relaxation Mechanisms in a Si/Si_xGe_{1-x} Quantum dot, Phys. Rev. Appl. **13**, 034068 (2020).
[37] P. Boross, G. Szechenyi, D. Culcer, and A. Palyi, Control of valley dynamics in silicon quantum dots in the presence of an interface step, Phys. Rev. B **94**, 035438 (2016).
[38] J. K. Gamble, M. A. Eriksson, S. N. Coppersmith, and M. Friesen, Disorder-induced valley-orbit hybrid states in Si quantum dots, Phys. Rev. B **88**, 035310 (2013).
[39] K. MacLean, S. Amasha, I. P. Radu, D. M. Zumbuhl, M. A. Kastner, M. P. Hanson, and A. C. Gossard, Energy-dependent Tunneling in a Quantum dot, Phys. Rev. Lett. **98**, 036802 (2007).
[40] N. Rohling, M. Russ, and G. Burkard, Hybrid Spin and Valley Quantum Computing with Singlet-Triplet Qubits, Phys. Rev. Lett. **113**, 176801 (2014).
[41] D. Culcer, A. L. Saraiva, B. Koiller, X. Hu, and S. D. Sarma, Valley-based Noise-Resistant Quantum Computation Using Si Quantum Dots, Phys. Rev. Lett. **108**, 126804 (2012).